

Harvard-Smithsonian Center for Astrophysics
Precision Astronomy Group

CONFIDENTIAL

For FAME Project Team only, competition sensitive.

To: Distribution 5 March 1999 TM99-02
From: J.D. Phillips
Subject: The FAME Error Budget.

In the 1998 MIDEX proposal for FAME^a [Johnston 98], the error budgets corresponding to Tables 1 and 6 of this memo are given (in Table FO1-3 and Table FO4-5, respectively). This memo gives an updated error budget, with derivations, including substantially lower error estimates for bright stars obtained by using a different method from that discussed in the MIDEX proposal. The current release (5 March '99) is a work in progress, distributed for the purposes of the FAME team as they carry out the current phase A study. Revisions will be necessary, and will be made in the coming weeks. Comments are solicited.

FAME's astrometric accuracy is shown in Table 1, and the systematic error budget is shown in Table 6. Error sources are divided into four parts: I. Stochastic, II. Internal systematic (errors due to the instrument), III. External systematic (errors that would affect an ideal instrument measuring at the same point in space), and IV. Intrinsic (e.g., motion due to resolved companions). Many of the internal errors vary systematically with parameters such as field position and position within the CCD chip. These errors will be well-studied. In a 2½ year mission there will be about 1.8×10^{11} observations in total, 1.1×10^{10} per chip, and 5.3×10^6 per CCD column. Each star is observed 270 times by each chip, and 4600 times^b by all (faint star) astrometric chips.

Laboratory characterization will determine the nature of the (larger of the) internal systematic errors and support parametric models, particularly of the optics and CCD's. However,

^a The design presented in the MIDEX proposal was an evolution of FAME-98 [Reasenberg and Phillips, 1998, Phillips and Reasenberg 1998]. For the MIDEX proposal, the orbit was changed from 100,000 km circular to geosynchronous. In the lower orbit, the solid angle subtended by the Earth is six times larger.

^b This number would increase by 20/17 if the current scheme for bright stars, in which 3 CCD chips have 97% attenuating filters over them, is replaced by one that makes more efficient use of the CCD's, such as a variant of the GAIA scheme in which the clock for a chip with a bright star on it is stopped except for brief intervals in which charge is accumulated, up to the limit imposed by well-filling. The number of bright-star observations would increase by 20/3. While bright stars are relatively few, they contribute importantly to the accuracy of the whole solution, and to determining instrument bias parameters.

before launch, it will not be possible to gather sufficient knowledge for the reduction of the on-orbit observations. Instead, the observations themselves will be used to refine the parameters of the pre-launch models and, where necessary, to add new parameters to model effects that were not discovered on the ground. This error budget has a number of terms, corresponding to statistical error and the various sources of systematic error. The *a priori* value of a term refers to the uncertainty that can be obtained from using the data of a single observation, as well as any information known independently of FAME (such as spectral type from an independent catalog). *A posteriori* refers to the uncertainty that can be obtained by employing all the mission data, astrometric and photometric, as well as ancillary data.

The vast dataset enumerated above will support the estimation of a large number of instrument parameters, in addition to the astrometric parameters (which will be much more numerous) [Phillips 1999]. Even if it were necessary to include in the model one or more parameters per CCD column, there are sufficient data to support the estimation.

The first component of FAME's error budget is stochastic error. Low stochastic error is a prerequisite for the investigation of other error sources. We have performed numerical experiments to evaluate FAME's centroiding precision (Phillips & Reasenberg 1998). We assumed a blackbody source and modelled the diffraction pattern accordingly, estimating along-scan position, magnitude, and the source temperature. For $V=9$ the precision is $540 \mu\text{as}$, and for $V=12.3$ it is $2500 \mu\text{as}$. This corresponds to $1/460$ of the half-width at null for $V=9$ and $1/100$ for $V=12.3$. In the laboratory and using stare mode, centroiding was demonstrated to comparable precision: $1/1200$ of the half-width at null with a circular aperture [Winter 1998]. The uncertainties as a fraction of a pixel are $1/770$ for FAME ($V=9$) and $1/500$ for the laboratory work. FAME uses TDI, which averages some types of error, while the lab work was done in stare mode.

Bright stars will overflow the CCD wells, causing charge to migrate (primarily along the column). The magnitude at which the wells overflow depends on whether the star falls at the center or edge of a pixel, and on the extent to which the observation is smeared laterally due to precession. (The number of columns over which precession spreads the image varies approximately sinusoidally over the ~ 10 day precession period, with amplitude 5 columns.) The range at which overflowing occurs is $7 < V < 9$. The accuracy for $V < 9$ is currently calculated assuming that 3 chips are covered with neutral density filters, and bright stars are measured only in those chips. The astrometric accuracy can be substantially improved in the magnitude range $V < 9$ by several techniques. Anti-blooming techniques may make it possible to precisely measure the wings of the PSF to obtain the star's position. Another technique is to briefly halt clocking just before a bright star comes onto the chip, then restart, then halt it again before the brightest pixel overfills. The accumulated image is accompanied by a uniformly-illuminated column before and after. (Note that the clock will be gated off only for the chip that is to detect the bright star, but that the other chips will continue to run normally.) The charge packet with shortened TDI is read out in the normal way. It is likely to be advantageous to halt the clocking

Table 1. FAME Mission Accuracy. The observations for $V=8$ are restricted to those that are sufficiently spread out by precession to avoid saturation. This restricted set of faint-star chip observations far outweighs the set from the bright-star chips. For $V \leq 7$ only the bright-star observations are available. The column "Transmitted to Horner" is calculated from the SAO covariance study, including the effects of read noise, Poisson statistics, and number of observations. To allow for unmodelled systematic error, $10 \mu\text{as}$ is added in quadrature to all mission error figures. The "In proposal" column gives mission accuracy values from the proposal. "TDI interrupted, once" is for the clock-gating scheme, in which the clock runs during a single interval while the bright star is on the chip. Some improvement for $5 \leq V \leq 8$ is possible by allowing longer integrations on stars spread out by precession. The actual "TDI interrupted, several \times " is for an extension of that scheme in which the clock runs for several distinct intervals while the bright star is on the chip, resulting in several separate measurements.

Visual Magnitude	MIDEX				TDI interrupted	
	Number of Observ'ns	Filter Transmission	Transmitted to Horner μas	In proposal μas	Once μas	Several \times μas
5	810	1/40	29	29	14	
6	810	1/40	44		14	
7	810	1/40	68	48	14	
8	1150	1	18		14	
9	4600	1	15	15	14	
10	4600	1	21		19	
11	4600	1	30	30	28	
12	4600	1	47		44	
13	4600	1	76	76	70	
14	4600	1	128		118	
15	4600	1	226	226	209	
16	4600	1	427		394	

multiple times. This technique cannot work for $V < 0$, at which brightness the well overfills while the image dwells on a single pixel. If either of the above two techniques or some other proves successful, the positional accuracy for $V < 9$ would improve.

There has not been a detailed study of additional error sources using the gated-clock scheme, but here are two, to start the list. 1) Electron traps will delay charge being transferred along a column. Some traps have a timescale comparable with the vertical shift time, so will shift some charge from the leading edge of the image to the trailing. If the TDI happens to stop the image on a trap, it will have time to release its charge.

In the remainder of this memo, I discuss the error budget shown in Table 6. The sections below are numbered to correspond to the lines of the table and to the outline of Appendix A.

I. A-B. Statistical Error. The values given here come from the SAO centroiding study [Phillips and Reasenber, 1998]. When the Modulation Transfer Function (MTF) of the CCD is taken into account, the error values will increase somewhat. (The study is underway, but on hold, at SAO as of 3/1/99.)

II.A.1. QE Variations. The analysis of bias due to QE variations of SAO TM97-01 applies to a CCD with TDI if the QE variations depend on the applied voltages, and thus move with the stellar image. QE variations that are fixed on the chip will be substantially averaged by TDI, and will be ignored here. Let the QE be multiplied by a factor $[1 + \alpha \sin(kp + \phi)]$, so that α is the fractional amplitude for the perturbation, k is its wavevector ($2\pi/\text{period}$), ϕ is its phase, and p is angle on the sky in the scan (sensitive) direction. Let f be the number of cycles of perturbation in

Table 2. Parameters for QE variation.

Parameter	Symbol	Value (FAME-98)
Perturbation amplitude	α	0.05
Pixel angular width	θ_p	0.413 arcsec
Perturbation wavevector	k	15.2 arcsec ⁻¹
Obscuration fractional width	γ here (now κ)	0.4

Table 3. *A priori* uncertainty in fraction of light between 800 and 900 nm, as a function of star temperature.

T, K	$\sigma(T)$, K	f8	df8/dT, K ⁻¹	$\sigma(f8)$
3000	14.8	0.378	126.10	0.00187
5777	50.9	0.191	32.42	0.00165
10000	170.1	0.122	8.03	0.00136
15000	417.3	0.097	2.84	0.00119
25000	1207.8	0.082	0.81	0.00098
35000	2286.4	0.077	0.37	0.00085

one Airy box, $2\lambda_o/S$ (TM97-01, p. 4), and n_s be the number of pixels per Airy box. For a perturbation whose period is one pixel, $f = n_s$, so $f = 1.2$. The fractional width of the obscuration, called here γ , is 0.4. (In more recent FAME writings, this quantity is called κ .) With these parameters we determine $G(\gamma, f)$ from Fig. 2 of TM97-01 (p. 5). G is -1. This value is exact in the case that an infinite extent of detector is read out. The position bias is

$$\Delta = \Delta_o \cos(\phi) \quad (1)$$

where

$$\Delta_o = \frac{3\alpha}{16\pi(1-\gamma^3)} \frac{\lambda}{S} G(\gamma, f) \quad (2)$$

(TM97-01, eq. 13). With the parameters given, summarized in Table 2, $\Delta_0 = 800$ microarcsec (μas). The rms variation of Δ over the observations of a star (i.e., ϕ goes from 0 to 2π) is $560 \mu\text{as}$.

To determine the level to which this bias can be modelled *a posteriori*, note that stars with $V=9$ have a single-measurement precision of $540 \mu\text{as}$. (It is purely coincidence that this precision is nearly the same as the rms value of the bias to be estimated. The value of the bias is unrelated to the accuracy with which it can be modelled, except that a large bias must be proportionately more stable if we are to avoid the need to model its time-variation.) Consider stars with $8.5 < V < 9.5$. Other spans of 1 magnitude will make comparable contributions to the determination of the CCD bias parameters; this advantage is neglected here. Each CCD makes $> 3 \times 10^7$ observations of stars with $8.5 < V < 9.5$. To estimate the above bias to an accuracy of $10 \mu\text{as}$ using observations with a precision of $540 \mu\text{as}$, we need ~ 3000 observations. We have at least four orders more observations than that. The extra observations could be used, if necessary, to model a QE variation that varied with time, or even to model a variation that was different for each CCD column. It seems reasonable that the CCD geometry will be stable with time. Also it is plausible that modelling on a column-by-column basis will not be needed: errors in the printing process used to make the CCD's will tend to vary smoothly from one pixel to the next, perhaps with flaws of a particular type such as the periodic steps in the __ CCD <<Shaklan et al. ref.>>. Clearly, laboratory study of the flight CCD's will be needed, with an emphasis on characterizing the type of defects, for example the periodic steps of Shaklan et al., rather than on measuring them all in the lab to an accuracy sufficient to correct the flight data. A model of the latter scope and accuracy is best derived from the on-orbit observations themselves. A preliminary look at the computation requirements for estimating one parameter per CCD column indicates that it is feasible with current hardware.

II.A.2.b. CCD Wavelength-Dependent Absorption. This effect arises because the optical system is not telecentric, so away from the center of the field, the beam impinges on the detector at an angle. The absorption length in the detector depends on wavelength, and therefore on the object's spectrum.

Let θ_f be the field angle (maximum astrometric field is 1.1°), f be the effective focal length (7.5 m), and d_p be the distance from the exit pupil to the detector (97 cm). Then the angle at which the beam impinges on the detector is

$$\theta_1 = \frac{f}{d_p} \theta_f = 8.5^\circ \quad (3)$$

This angle is reduced when the beam enters the silicon. Taking the index to be 3.5 and the thickness $25 \mu\text{m}$, the lateral travel is $2 \mu\text{m}$. The photons are detected throughout the thickness. For wavelengths longer than 800 nm, a substantial fraction of the photons penetrate the 15-18 micron thickness of the CCD [Bates, priv. comm. 1998]. Photons that penetrate the entire thickness have an average offset of half the maximum given above, i.e., $1 \mu\text{m}$ or 30 milliarcsec (mas). When averaged over wavelength, the shift depends on the fraction of photons in the band from 800 nm to the long wavelength limit (here taken to be 900 nm).

A priori, the temperature of a V=9 star can be known to an uncertainty $\sigma(T)$ (Table 3) from determination of the apparent width of a single observation. The effect of a non-perpendicular beam depends on f_8 , the fraction of the star's radiation detected by FAME that is in the band from 800 to 900 nm. The effect on temperature is proportional to the derivative of f_8 with respect to temperature. From Table 3, the *a priori* error in f_8 is <0.002 , so the *a priori* angle bias is $<55 \mu\text{s}$. Furthermore, the bias would cancel in the average of the two or three observations of a single passage across the focal plane due to the symmetry of the CCD layout (see below).

A posteriori, the 4600 determinations of temperature of the star can be used to improve the temperature estimate, as well as the 1080 photometric observations. The abundance of observations imply that even a variable star's spectrum can be characterized adequately. The expected *a posteriori* angle bias is $<1 \mu\text{s}$.

Symmetry of CCD layout. Several biases depend on field angle. There is a substantial reduction of the effect because of the symmetry with which the detectors are laid out. Consider scan and cross-scan axes in the focal plane (Fig. _). Flipping the up-scan part of the focal plane to down-scan would be a reflection in the cross-scan axis. A star that crosses the focal plane is observed in two or three CCD's, and these are symmetrically laid out in both scan and cross-scan. If asymmetrical CCD layouts are considered, consideration should be made of the systematic error consequences. It must be pointed out that the symmetry should not be relied upon too heavily: some observations will inevitably be asymmetrical due to bad CCD columns, or even the failure of a whole chip.

II.A.2.d. Fringing. The bias due to fringing in the CCD still needs to be accounted for. An error due to fringing in an up-scan chip will be accompanied, to first order, by an equal and opposite error in the down-scan chip. If the star crosses a chip that is on the cross-scan axis, the fringing effect is cancelled within the chip itself. This cancellation is imperfect if the fringing is different in the two chips, or in the up-scan and down-scan portions of a single centered chip. Differences in the fringing will arise due to variations in CCD thickness and to variations in the absorption length.

II.A.3.b. Charge Transfer Effects -- Along-column bleed near full-well. In the laboratory centroiding experiments [Winter 1998], charge transfer effects due to well-filling lead to a bias of approximately 1/500 pixel. Winter says that he did not adjust his PSF for well-filling. Also, his PSF was obtained from an average of many of his standard observations, rather than by adjusting the parameters of a theoretical PSF, or from a PSF measured at higher magnification. This average empirical PSF may have resulted in further biases. Therefore, the 1/500 pixel result should not be interpreted as a universal limit.

A priori. Taking Winter's results at face value, for FAME 1/500 pixel is $800 \mu\text{s}$. This effect will be largely repeatable, with a component that depends on the phase of the observation with respect to the pixels. The phase of the 4600 observations of one star will be uniformly distributed. The bias due to well-filling may however have a component that always tends to retard the star in the scan direction. This systematic component is likely to depend on which column the observation falls in, and may depend to some extent on the stellar spectrum. If we

only require that we model these effects to ~10%, the large number of data available are likely to support the creation of a sufficiently accurate model. Therefore, the *a posteriori* error will be no more than 80 μas .

II.A.3.d. Charge traps. An effect that will vary from column to column is trapping, which will affect charge transfer, moving collected electrons from the leading edge of the image toward the trailing. Columns with one or more traps will have an additional contribution to the astrometric error. This contribution may depend on temperature, if the trap parameters do. Traps tend to hold a few electrons, and some hold them long enough to create a delay in the along-column (2.5 kHz) shift. If the depth and lifetime vary with CCD temperature, there will be a varying bias in columns with traps. If 10 electrons are shifted from the leading edge of a full-well ($V \sim 9$) image (which has 10^5 electrons) to the trailing, the *a priori* shift is 10^{-4} pixel, or 40 μas . However, for an image near the faintest magnitude, say 16.5, the effect is more important. *A posteriori*, the shift due to a column with a trap can be estimated to extremely high accuracy as long as it is stable. The effects that will make traps vary are temperature <<radiation creates traps? Might contamination change a trap?>>. <<How many traps do we expect to have to estimate parameters for: much less than one per column?>>

Table 4. Uncertainties in a three-parameter fit for angle, magnitude, and temperature. Results are derived from an average of the information matrix over pixel phase. Apparent magnitude has been held constant at $V=9$ by adjusting bolometric magnitude. The correlation coefficient between magnitude and temperature is c_{23} . (Correlation coefficients between angle and magnitude, and angle and temperature, averaged over pixel phase, are zero to within computational accuracy, as they must be by symmetry.) From SAO covariance study.

Temp, K	$\sigma(\theta)$, μas	$\sigma(\text{mag})$	$\sigma(T)$, K	c_{23}	m_{bol}
3000	373	14.1	14	-0.9960	7.10
5777	532	2.1	50	-0.4253	8.90
10000	524	21.7	159	0.9958	8.64
15000	485	51.8	379	0.9993	7.85
25000	421	110.8	1076	0.9999	6.40
35000	377	161.7	2030	1.0000	5.27

II.B.1. Incorrect stellar spectrum model. The position of a star symmetrically located with respect to the pixels could be estimated without knowing the width of the image. However, in almost all cases a knowledge of the width, shape, and amplitude of the distribution is essential.

For a solar-type star, our covariance study of centroiding has shown that the temperature of a black body equivalent to a $V=9$ star at 5777°K can be determined to 1% in a single observation [Phillips and Reasenberg, 1998]. Stars that are much hotter have less well-determined temperature, but for those stars, the portion of the spectrum that falls within the FAME passband is similar, so this larger fractional uncertainty in temperature does not indicate large unknown variations in spectrum, so unknown biases in angle. In fact, the covariance study shows that when V magnitude is held constant, the angle uncertainty when fitting stellar temperature is largely unchanging.

With this information about the spectrum, it is reasonable that the position can be determined *a priori* to 1/100 pixel. The mission error on position can be as low as 15 μas . Here I assume that

the temperature can be determined well enough that the error in the spectrum model contributes less than three times this error, i.e., about 50 μas . <<?? reasoning for this?>>

Work is underway at SAO on fitting real stellar spectra both with appropriate model spectra whose parameters are estimated, and with model spectra that are deliberately inappropriate.

II.B.2. Undetected companions. Companions are detected by FAME with surprisingly high sensitivity by examining the apparent width of the image in all directions, using all data from the mission: separations as small as $\sim 250 \mu\text{as}$ <<check Δm range>> can be detected (see below). If undetected, however, a companion causes a shift in the center of light. Two or more objects whose orbital motion over the course of the mission is significant must be reduced as a single multicomponent model in stage VI of data analysis (catalog creation). It may be just possible for companions to be close enough to have significant orbital motion, yet sufficiently separated that the images are separate and would ordinarily generate separate "postage stamps" of detector pixels read out. For example, a binary of separation 10 AU at 10 pc has an apparent separation of 1 arcsec. Its motion would be extremely well-measured, so the small departure from linearity of motion might be significant. <<easy calculation - do it.>>

Detected companions can be modelled, and positions for all stars of the system derived, probably to an accuracy comparable with that obtainable if they were single stars, except for the effect of shot noise from an overlapping image of comparable or greater brightness. <<This is a POINTS result. Do we have substantiation useful in the context of FAME?>> An undetected companion will bias the estimates of position and proper motion, and to a lesser extent, parallax. The shift of the center of light, for a system with the maximum undetected separation, is $\sim 1/4$ of the separation or 60 μas , and occurs when the magnitude difference is ~ 2.9 .

To detect a companion, we use all estimates for the image width of that object over the entire mission. The width of the image, i.e., effective temperature, can be estimated for a $V=9$ star to within 1% in a single measurement (Phillips & Reasenberg 1998). Since the width is $\sim 300 \text{ mas}$, the single-measurement precision is 3 mas. Roughly half of the ~ 4600 measurements can be used to get image widths in two orthogonal directions^c, so the mission precision is $\sim 60 \mu\text{as}$. For systems with separation of the components greater than $\sim 250 \mu\text{as}$ <<arbitrary>>, modeling of the Point Spread Function (PSF) will detect the companion, and positions will be estimated separately for both.

Orbits with period less than $0.8\times$ the mission duration will also be detected in the position residuals, and longer-period orbits with substantially less sensitivity [Reasenberg, et al., in prep.]. Systems with separation and magnitude such that they escape detection, yet a large enough shift of the center of light to be a significant error source, will constitute a source of error. <<This is 10's or 100's of μas for stars in a quite small volume of parameter space. More work needed.>>

^c There is nothing magic about two directions: one could take hundreds of directions and build up a crude image in analogy with the tomography in medical imaging.

II.B.3. Onboard clock error. *A priori.* A good clock is readily available, so this error budget item can be specified so that the clock will be a completely insignificant contribution. The specification may be revisited if the clock proves more of a problem. A possible clock is the EMXO series of oven-stabilized quartz crystal oscillators made by Vectron Laboratories, Norwalk, CT. <<I think better oscillators are available for a comparable price - \$20-30K. Much better crystal oscillators are available for a much higher price, \$200-300K, from Johns Hopkins University Applied Physics Laboratory. These latter devices have no cost advantage over Rb or Cs masers.>>

Table 5. Ball EMXO clock stability.

τ , sec	root Allan var.	Time root var., sec	Equiv. angular root var., μs
0.1	1×10^{-11}	10^{-12}	0.001
1.0	1×10^{-11}	10^{-11}	0.01
10	5×10^{-12}	5×10^{-11}	0.05
500	$3.5 \times 10^{-11*}$	$1.8 \times 10^{-8*}$	19*

*Assuming that the Allan variance for $\tau > 10$ sec degrades as $\tau^{1/2}$.

Error in the onboard clock is equivalent to a rotation variation, and can be modelled as such. In principle, the onboard clock might vary rapidly compared with the rotation rate. The EMXO oscillator, however, has the short-term stability given in Table 5, which shows that the variance on long time scales is most important. (The temporal behavior of the EMXO is probably typical for ovenized quartz resonators.)

A posteriori. The clock error over one rotation will be estimated with data from the 10^4 stars with $9 < V < 11$ observed during that rotation. For these observations, the photon-statistics-limited error is 1300 μs . The clock error can therefore be estimated to about 13 μs . This is consistent with the uncertainty of estimating rotation parameters [Chandler and Reasenberg, in prep.].

II.C.1. Telescope geometry changes. Lockheed's text in the proposal stated that no part of the FAME instrument optics or structure would change temperature from its nominal by more than 5 mK. With a temperature coefficient for low-expansion GrCy of $10^{-7}/\text{K}$, this implies $\sim 100 \mu\text{s}$ error. This is likely to vary smoothly over a rotation, and could in that case be readily removed by modelling. A tilt of an element would appear as a drift in the basic angle, for example, and would affect all $\sim 10^3$ stars of $V < 10$ measured in that rotation. Therefore, geometry changes are likely to be modellable to better than 10 μs .

II.C.2. Optical distortion.

II.C.6. Refraction in CCD cover plate.

II.D.1.a. Rotation rate changes – fuel sloshing. For the MIDEX proposal, a N_2H_4 propellant system has been specified, which raises the possibility of torques due to sloshing. No estimates of these torques are currently available, so this error source is not treated here. Also, no attempt is made here to quantify spurious rotation due to leaking of the fuel through the nozzles, which

has been a problem on previous spacecraft with low-thrust requirements <<refs, e.g. to ranging experiments?>>

II.D.1.b. Rotation rate changes – Solar torque. *A priori.* The Sun acting on an azimuthally symmetric shield causes no torque about the rotation axis. However, small variations in shield reflectivity cause a substantial torque. These are expected to vary slowly over the mission, and to cause a sinusoidal variation in azimuthal angle; thus they are expected to be modellable. The *a priori* effect, however, is large.

First take the solar shield to be flat. Consider a patch of the shield whose reflectivity is smaller than the average by $\Delta R = 0.01$, whose area is $A_{\text{patch}} = 1 \text{ m}^2$, and which is centered $r_{\text{patch}} = 1 \text{ m}$ from the rotation axis,. The Solar radiation pressure on an absorbing surface at 1 AU from the Sun is $Q = 4.54 \times 10^{-6} \text{ kg m}^{-1} \text{ sec}^{-2}$ [Allen, 1976, p. 161]. The spacecraft moment of inertia about the rotation axis is 200 kg m^2 <<Mook, memo of 1998?>>. The force along the (anti-)Sun direction is

$$F_o = Q A_{\text{patch}} \cos(\xi) \Delta R_{\text{patch}} \quad (4)$$

where $\xi = 45^\circ$ is the angle between the Sun direction and the spin axis. The force perpendicular to the spin axis is

$$F = F_o \sin(\xi) . \quad (5)$$

and the torque about the spin axis is

$$\tau = F r_{\text{patch}} \sin(\varphi) \quad (6)$$

where φ is the angle of rotation about the spin axis. The angular acceleration is

$$\alpha = \frac{\tau}{I} = \alpha_o \sin(\varphi) \quad (7)$$

where

$$\alpha_o = \frac{Q A_{\text{patch}} \Delta R_{\text{patch}} r_{\text{patch}}}{I} \cos(\xi) \sin(\xi) . \quad (8)$$

The angular perturbation is

$$\Delta\varphi = \int_{t_o}^t \int_{t_o}^{t'} \alpha_o \sin\left(2\pi \frac{t''}{P}\right) dt'' dt' = -\frac{P^2 \alpha_o}{4\pi^2} (1 + \sin x) , \quad (9)$$

where in the second equation, $x = 2\pi t/P$, and t_o has been chosen to be $-P/2$. The rms angular departure from rotation at a constant rate is $P^2 \alpha_o / (4\sqrt{2} \pi^2)$, which is 0.6 arcsec for the parameters given above. The *a priori* bias is almost five orders of magnitude larger than the permissible *a posteriori* bias.

Since the effect of a single patch (of arbitrary size) on a *flat* shield is to cause a purely sinusoidal angular perturbation at the rotation frequency, the effect of all such reflectivity

variations will also be a single sinusoid at the rotation frequency, with only two parameters to be determined: amplitude and phase. There are other effects that can cause other types of perturbation. If the shield is conical instead of flat, for example, the projected area of the above patch will vary over the rotation, and the perturbation will no longer be sinusoidal.

A posteriori. A variation in rotation is much like a variation in onboard clock frequency, discussed above. The variation due to solar radiation pressure on a flat shield has two parameters, the amplitude and phase of the angular perturbation. (There would be small additional effects, resulting in additional parameters to be determined, if the shield and solar power array are not quite flat.) The discussion of clock error above shows that a single parameter, the rotation rate, can be estimated to $\sim 13 \mu\text{s}$ from the data of a single rotation. There were 10^4 data used for this estimate. Because the number of data is large, a substantial number of additional <<sufficiently non-degenerate>> parameters can be estimated to comparable accuracy, with little degradation in the accuracy of the science parameters. <<Phillips is to get first of Solar data about 3/8/99; more is available from the VIRGO instrument on SOHO, but it is ESO data, and ESO is reluctant to release it. I am trying various avenues for obtaining it.>>

II.D.1.c. Rotation due to Earth light shining in the ports. *A priori.* The Earth is less bright than the Sun, but shines directly into the view ports during a portion of each rotation at two epochs per orbit. The flux emitted by the Earth is $F_E = 340 \text{ watt/m}^2$. At the MIDEX altitude of 35786 km, the geometric coupling factor <<define>> is 0.023. Take the port area to be $A_p = 0.2 \text{ m}^2$ (larger than the actual beam at the aperture to allow for beam clearance). Assume that the port lies at 45° to the radiation, which is the angle at which torque is likely to be maximized, depending on the geometry of the surface the light happens to strike inside the instrument.

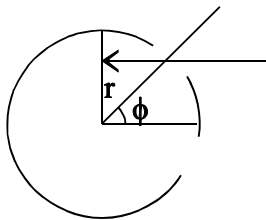


Figure 1. Earth light and port geometry.

The power coming in is 1.1 watt. This power exerts a force of 4×10^{-9} newton, which acts at a radius of $\sim 1 \text{ m}$, at an angle ϕ (Fig. _) of $\sim 60^\circ$, creating an angular acceleration of $2 \mu\text{s}/\text{sec}^2$. Supposing that this acceleration has a duration of 45° of rotation, it causes a perturbation of 20 mas. This perturbation will be difficult to predict well, since it depends on which structures within the spacecraft are struck by the Earth radiation, which may vary somewhat from rotation to rotation. Its overall amplitude also depends on the weather on Earth, and on the fraction of the side exposed to the spacecraft which is sunlit.

A posteriori. Observations will be used to model this effect to an accuracy comparable to that for the solar torque, but depending on how well it is possible to fit data from several adjacent rotations with a single model, it may require a significant increase in the number of parameters to be determined.

II.E. Imperfectly-determined grid. There had been no data reduction errors *per se*, as they are things like centroiding with the wrong model of the PSF or spectrum, and are included under other error budget items.

February 21, 1999: I have put in reduction errors in the spiral and global stages, but are these any more than *a posteriori* reflections of the perturbations such as Earthlight shining in the ports?

For starters, what drives the errors John sees in his study? I think it's no more than the Gaussian errors on the stellar observations. If correlations create larger errors in the spiral and global models than one would calculate via \sqrt{N} , I think they deserve a position in the error budget.

III.A. Ephemeris.

To correct for stellar aberration, the spacecraft velocity must be known. A velocity error of 1 cm/sec causes a $7 \mu\text{as}$ error in the aberration correction. The spacecraft velocity would vary on the timescale of the orbital period, 4 days so that the bias due to velocity error would be the same for N observations, and could be estimated to $50 \mu\text{as}/\sqrt{N} =$

Table 6. Error Budget - Single Measurement

§	Source	Error (microarcsec) [1]		Notes
		<i>a priori</i>	<i>a posteriori</i>	
I.A.	Photon Statistics • V=9	540	540	(1) <i>A priori</i> and <i>a posteriori</i> refer to the error before and after modeling (fitting) using iterative astrometric data reductions. The <i>a posteriori</i> errors are dominated by photon statistics, and all will be largely uncorrelated from one epoch to another. To arrive at the values in [Table 1], the photon statistics plus residual errors are divided by the square root of the number of measurements, with a small quantity added in quadrature (10 microarcsec) to account for correlations.
I.A.	• V=15	10800	10800	
I.B.	• Read noise, 7 e - rms, V=15	6600	6600	
II.A.1	QE Variation	560	<10	(2) Due primarily to Solar radiation pressure on the shield, whose reflectivity varies spatially (we assume 1% over 1 m ²). The rotation error varies smoothly over a rotation, and changes very little from one rotation to the next. Therefore, it can be modeled to very high accuracy. Somewhat more difficult to model is the rotation error due to Earth radiation (reflected and reradiated) entering the viewports, which causes a rotation variation of order 20 μas, but the torque varies according to which instrument structures are illuminated, and the weather on Earth. Data from a single rotation suffice to model the spacecraft attitude to the level shown.
II.A.2.b.	CCD Wavelength-Dependent Absorption	300	30	
II.A.3.	Charge Transfer Effects	800	80	
II.B.1.	Incorrect Stellar Spectrum Model	4000	50	
II.B.2.	Undetected Companions	60	60	
II.B.3	Onboard Clock Error	<10	<1	
II.C.1.	Telescope Geometry Changes	100	<10	
II.C.2	Optical Distortion	2000	20	
II.C.6.	Refraction in CCD Cover Plate	1	<1	
II.D.1.	Rotation Rate Changes	10 ⁶ [2]	<1	
III.A.	Ephemeris (1 cm/sec knowledge)	7	<1	

Appendix A. FAME error budget, outline form

Note that Fringing has recently moved from II.A.1.f to II.A.2.d.

I. Statistical error

- A. Photon statistics, $V=12.3$, position: single-measurement (mission), $\mu\text{as} \dots 2400$ (50)
- B. Read noise & dark current. $7 e^-$ rms raises the variance a factor two for a star of $V=15$.

II. Internal systematic error.

A. CCD Errors.

- 1. QE variations.
 - a. Intra-pixel variations that move with accumulating charge.
 - b. Inter-pixel.
 - c. Wavelength-dependent.
 - d. Non-linearity.
 - e. Bad pixels & columns.
- 2. Detection of photons in the wrong pixel.
 - a. Fixed on chip.
 - b. Beam non-perpendicular, with wavelength variation of absorption.
 - c. Dependence of Modulation Transfer Function (MTF) on wavelength.
 - d. Fringing (in red).
- 3. Charge transfer effects.
 - a. Efficiency (CTE) in the wake of a bright star.
 - b. Along-column bleed when approaching full-well.
 - c. Deterioration due to radiation damage.
 - d. Charge traps.
- 4. Electronics.
- 5. Physical flatness.
- 6. Recovery from saturation.

B. Centroiding.

- 1. Incorrect stellar spectrum model.
 - a. Error in estimation of spectral type.
 - b. Metallicity effects.
 - c. Reddening.
 - d. Non-stellar objects.
- 2. Unresolved companions.
- 3. Onboard clock error 0

C. Optics.

- 1. Element shape, spacing, and orientation changes, including changes in the basic angle.
 - a. Thermal.
 - b. Long-term drift, e.g., water loss. 0
- 2. Aberration-induced shift of centroid varies with field.

- a. Gain variation between columns changes emphasis on the advanced portion of the wing of the image. 0
 - 3. Need to determine the PSF.
 - 4. PSF varies with field.
 - 5. Non-uniformity of mirror reflectivity varies with time (and PSF is not symmetrical.) 0
 - 6. Temperature difference in CCD cover or a Gascoigne plate, combined with dn/dT .
 - 7. Contamination of CCD or its cover.
 - 8. Cosmic rays.
 - 9. Scattered light.
- D. Rotation.
 - 1. Spin rate changes.
 - a. Viscosity of station-keeping fuel slows the rotation.
 - b. Patch on the solar shield has different reflectivity.
 - c. Earthlight shining in ports - variable torque.
- E. Imperfectly-determined "grid".
 - 1. Rotation spiral model errors. (This has no *a priori* component.)
 - 2. Global model errors. (This has no *a priori* component.)
- III. External systematic error.
 - A. Ephemeris. 0
- IV. Intrinsic error, or signal.
 - A. Motion due to resolved companions.
 - B. Stellar activity.

References

Bates, Phil, Lockheed Martin Co., stated by telephone in Fall, 1998 that the LMCO CCD's under consideration for FAME are 15-18 μm thick.

Johnston, K.J. "Full-Sky Astrometric Mapping Explorer (FAME)", Proposal to NASA's Explorer Program, Medium-Class Explorers (MIDEX) and Missions of Opportunity, Aug. __, 1998

Phillips, J.D., and R.D. Reasenberg, "Optical System for an Astrometric Survey from Space", Proc. of Conference 3356 on Space Telescopes and Instruments V, Kona, HI, SPIE (1998).

Reasenberg, R.D., and J.D. Phillips, "Design of a Spaceborne Astrometric Survey Instrument", Proc. of Conference 3356 on Space Telescopes and Instruments V, Kona, HI, SPIE (1998).

Reasenberg, R.D., R.W. Babcock, and J.D. Phillips, "An Astrometric Planet Search, Simulations and Mission Characteristics", in preparation, 1999.

Phillips, J.D., "Parameters to be estimated in FAME data reduction", SAO/PAG Technical Memorandum, in preparation (1999).

Winter, L., private communication, 1998. Based on work towards a thesis at the Hamburg Observatory. <<W. van Altena will try to ask Winter or C. DeVegt about this work when in Germany 3/4/99, ..., especially to see if there is something written that we may cite, or at least read.>>

Distribution

R. Babcock
J. Chandler
R. Reasenberg
I. Shapiro
FAME Web page *via* S. Horner